

Structural design of pavements incorporating foamed bitumen mixtures

Kranthi Kuna BE, MTech, PhD

Pavement Engineer, Mott MacDonald Ltd, Southampton, UK
(corresponding author: kranthi.kuna@mottmac.com)

Gordon Airey BSc, MSc, PhD, CEng, MICE

Professor, The University of Nottingham, Nottingham, UK

Nick Thom BSc, PhD, CEng, MICE

Assistant Professor, The University of Nottingham, Nottingham, UK

This paper presents a rational structural design methodology termed the 'cumulative damage approach' for road, port and airport pavements incorporating cold bituminous mixtures with foamed bitumen. This has been developed along with a laboratory test, the uniaxial indirect tensile test, to evaluate the fatigue characteristics of these mixtures. The test was developed with a view to addressing the limitations of conventional fatigue tests for foamed bitumen mixtures. The new design approach takes account of the actual stiffness evolution of the mixtures obtained from the fatigue test. It is compared with a traditional approach for conventional flexible pavements, which is based on pavement life as a function of computed tensile strain in the material and interpretation of fatigue data in a conventional way. The results show that the traditional design approach yields conservative outcomes for pavements with foamed bitumen mixtures if the same transfer function or shift factor used for hot mix asphalt is applied. The results also show that if all factors other than induced load influence are the same, the shift factor for foamed bitumen mixtures could be 25–35% higher than for hot mix asphalt.

Notation

| | |
|---------------------|--|
| C, m | regression constants for fatigue equation |
| K | shift factor that accounts for all the factors that influence pavement performance |
| K_L | shift factor that accounts for the load induced damage |
| k_1, k_2 | regression constants for k - θ model |
| N | pavement design life |
| N_{design} | design number of gyrations in gyratory compactor |
| N_f | number of load applications to failure |
| n | number of time intervals for pavement life |
| S | stiffness modulus |
| ε_i | tensile strain at the bottom of base for a constant stiffness in interval i |
| ε_t | tensile strain at the bottom of the asphalt layer |
| θ | bulk stress |
| σ_c | confining stress in triaxial test |
| σ_d | deviator stress in triaxial test |

1. Introduction

The structural design of road, port and airport pavements is required to make sure that the structure performs structurally and functionally in an economically viable manner for the designed life period. However, this task of designing a pavement structure is not as straightforward as for some other engineering structures. Moreover, there is never a unique design for any combination of design inputs (Thom, 2013). The major issue regarding the design of pavement structures is developing a useful relationship between the laboratory

performance and the field performance of the materials used in the pavement. The mechanistic–empirical method, which is based on the mechanics of the materials and relates an input such as wheel load to an output (pavement layer response) such as stress or strain, is a possible option. This paper applies this mechanistic–empirical approach to the design of pavements incorporating cold bituminous mixtures with foamed bitumen (foamed bitumen mixtures). The scope of the study is limited to design based on the fatigue criterion only.

The indirect tensile fatigue test is a widely used test method for hot mix asphalt in the UK. The major reason for the wide acceptance of the indirect tensile fatigue test over other tests is that it is simple and less expensive and, more importantly, that cores from in-service pavements can be tested. A major assumption in the indirect tensile fatigue test is the linear elasticity of the materials. As foamed bituminous mixtures are found to behave non-linearly even at small stress/strain levels, the actual stress distribution is complex (Jenkins, 2000; Kim, 2009). This brings into question the use of the indirect tensile fatigue test as a performance indicator for foamed bituminous mixtures. Past research findings also suggest that the indirect tensile fatigue test is too conservative a test for evaluating the fatigue life of cold bituminous mixtures due to their high void content (Jenkins *et al.*, 2002; Van de Ven *et al.*, 2007). Furthermore, for cold bituminous mixtures it is difficult to manufacture beams for beam fatigue tests (Long and Theyse, 2004; Long *et al.*, 2002; Ramanujam and Jones, 2007). Even if foamed bituminous mixture beams have been made without

Offprint provided courtesy of www.icevirtuallibrary.com
Author copy for personal use, not for distribution

excessive aggregate loss during saw cutting, the variability of test results has been found to be very high using beam fatigue tests (Long *et al.*, 2002; Ramanujam and Jones, 2007). In view of these limitations of the applicability of indirect tensile fatigue tests and beam fatigue tests to foamed bituminous mixtures, in this study the applicability of the uniaxial compression test was studied. This test was chosen as it has less complex stress conditions compared with other tests such as the indirect tensile fatigue test and flexural beam tests. In addition, test specimens can be prepared from a core taken from an in-service pavement for validating the in-service condition of a pavement layer.

2. Materials and methods

As can be seen from Table 1, a total of three foamed bituminous mixture types were considered in this study. Two with 50% reclaimed asphalt pavement (RAP) aggregate and one with 75% of RAP content. About 1% cement was added to one of the 50% RAP mixtures and to the 75% RAP mixture. A conventional hot mix asphalt, which was a dense binder course recipe mixture with 90 pen bitumen (DBM90), was also included in the study for comparison. Hot mix asphalt specimens were manufactured in a gyratory compactor in accordance with the specifications outlined in BS 4987-1:2005 (BSI, 2005) with 20 mm maximum aggregate size, and the bitumen used was the same bitumen as used in the foamed bituminous mixtures. Table 1 presents the key mix design parameters, namely mixing water content (MWC), foamed bitumen content (FBC) and the design number of gyrations (N_{design}) that were adopted in the study. These parameters were obtained from a mix design study carried out on these mixtures without cement. The details of the procedure adopted to identify these mix design parameters can be found elsewhere (Kuna, 2014; Kuna *et al.*, 2014). It was assumed that the addition of cement would not significantly influence the optimum MWC, FBC and design number of gyrations (N_{design}) in the gyratory compactor. Therefore, the same parameters that were obtained in the study for mixtures without cement were adopted for mixtures with 1% cement. The cement used in the study was ordinary Portland cement. For brevity, the physical properties of the component materials used in the study are not presented in this paper. Details can be found elsewhere (Kuna *et al.*, 2014, 2016).

Both the mechanistic–empirical pavement design approaches discussed in this study use a multi-layer linear elastic model to

Table 1. Mix design parameters adopted in the study

| | MWC: % | FBC: % | N_{design} |
|---------------------|--------|--------|---------------------|
| 50% RAP | 4.8 | 3.25 | 110 |
| 50% RAP + 1% cement | 4.8 | 3.25 | 110 |
| 75% RAP + 1% cement | 4.8 | 3 | 100 |

calculate the pavement response to a standard wheel load configuration. The standard wheel load adopted was a 40 kN single wheel load with a contact radius of 0.136 m with a uniform vertical stress of 690 kPa. The 40 kN load follows the recommendations by Highways England (HD 26/06 (HA, 2006)) on alternative pavement design procedures. However, the contact radius is smaller than the HD 26/06 recommendation of 0.151 m. This smaller value is chosen to induce higher stresses in the hypothetical structure and thus to study the effect of the non-linearity of foamed bituminous mixtures on pavement design. A hypothetical pavement structure was assumed for study purposes. The pavement consists of 50 mm of surfacing, 200 mm of base (and binder course) and 200 mm of sub-base over a subgrade of 15% CBR (California Bearing Ratio). The foundation (subgrade + sub-base) is in line with the class 2 foundation type in accordance with Highways England foundation design guidance (IAN, 2006). The comparative study of the two pavement design approaches has been carried out considering the base material (three foamed bituminous mixture types and one hot mix asphalt type) as a variable and all other parameters as constants.

3. Uniaxial indirect tensile fatigue test

The uniaxial indirect tensile test comprises the application of a sinusoidal (haversine) load on a 100 mm high \times 100 mm dia. cylindrical specimen in the axial direction at a frequency of 1 Hz. As a very low-friction system is provided between loading plates and specimen, giving a near uniaxial stress condition, the principal failure plane will be parallel to the stress direction and the principal strain is perpendicular to the failure plane. Therefore, the testing involves application of high compressive stress levels so as to induce significantly high radial strains such that the test is completed within a reasonable length of time.

3.1 Test set-up

The test apparatus used for applying the sinusoidal load consisted of an Instron loading frame, a 100 kN servo-hydraulic actuator with ± 50 mm movement, an axially mounted load cell and a temperature-controlled cabinet mounted on the loading frame. Rubicon software, which is a digital servo-control system, was used for operating the loading frame and for data acquisition.

The sinusoidal load of 1 Hz frequency was applied on the specimen through two loading plates (top and bottom). During the test, the axial and radial deformations were measured by axial and radial linear variable displacement transformers (LVDTs). The LVDTs for axial deformation measurement were placed on the top platen (Figure 1). These vertical LVDTs were fixed to magnetic supporting arms. The axial deformation was taken to be the average of the two axial

Offprint provided courtesy of www.icevirtuallibrary.com
Author copy for personal use, not for distribution



Figure 1. Test set-up for uniaxial indirect tension test

LVDT measurements. The radial deformation of the specimen during the test was measured with an LVDT fixed to a collar that was mounted at the mid-height of the specimen. The range of the horizontal LVDT was ± 10 mm and it was calibrated to measure the radial deformation of the specimen directly.

Since the aim of the test was to induce radial tensile strain along the height of the specimen, it was important to have uniform radial deformation throughout the height of the specimen. To ensure this, a friction-reducing system was used between the specimen and the loading plate. The system consisted of a 50 μ m polyethylene foil in combination with a thin layer of silicon compound, a grease-like material made by Dow Corning, between the foil and the specimen. The major problem experienced from using this friction-reducing system was the sliding of the specimen during the test, which could potentially have caused damage to the instrumentation, particularly to the collar for horizontal deformation measurement. Therefore, care needed to be taken while testing to make sure that the system did not slide.

After setting up the test specimen as explained above, tests were carried out under controlled stress conditions. Stress

levels were selected in order to give as wide a range of failure lives as possible. Table 2 shows the range of stresses applied to the specimen and the resulting initial horizontal (radial) strain values. The initial strain values were the average values of radial recoverable (peak to peak) strains over the first ten cycles of the test. Before the start of the test, a compressive holding load (pre-load) of 10 N was applied to the specimen to make sure it was held stably during the test. Following the pre-loading, the sinusoidal target load was applied to the specimen. Visual inspection of the specimen during the test revealed that, above a radial deformation of 5 mm (5% radial strain), the specimen had wide vertical cracks (Figure 2) and the axial strain increased at a rapid rate that could damage the instrumentation. Therefore, the test was stopped once the total horizontal deformation reached a radial strain of 5%.

3.2 Fatigue criterion

An advantage of this test over the indirect tensile fatigue test is that the failure characteristics (stiffness, permanent deformation and so on) can be monitored during the test. In this study, the failure criterion used was the reduction of the initial stiffness to 50% (50% retained stiffness), which was assumed to coincide with complete failure. Figure 3 shows fatigue lines plotted as initial strain against number of cycles to reach 50% stiffness. Linear regression was carried out on the data points obtained for each mixture to fit the model in Equation 1. The corresponding coefficients obtained after the fitting are tabulated in Table 3. R^2 values from the table suggest that the data collected for each mixture fitted the fatigue equation very well. Figure 3 demonstrates that the differences in fatigue life among the mixtures considered in the study were fairly small, particularly at lower initial strain levels. These laboratory tests employed sinusoidal loading of 1 Hz (stress controlled). In practice, these loadings are distributed across the pavement and there are also rest periods between wheel loadings. To accommodate these effects, a correction factor called a shift factor (or transfer function) is usually applied to the fatigue equation to be used in pavement design

$$1. \quad N_f = C \times \left(\frac{1}{\varepsilon_t} \right)^m$$

Table 2. Range of applied stresses and resulting initial radial strains for fatigue tests

| Target stress level range and corresponding initial strain range | | |
|--|-------------------|---|
| Mixture type | Stress range: kPa | Initial radial strain range: $\mu\varepsilon$ |
| 50% RAP-foamed bituminous mixture | 600–2100 | 78–421 |
| 50% RAP + 1% cement-foamed bituminous mixture | 800–2400 | 96–384 |
| 75% RAP + 1% cement-foamed bituminous mixture | 800–2400 | 78–381 |
| DBM90-hot mix asphalt | 1000–3000 | 86–550 |

Offprint provided courtesy of www.icevirtuallibrary.com
Author copy for personal use, not for distribution



Figure 2. Foamed bituminous mixture and DBM90 samples after testing

where N_f is the number of load applications for failure, ϵ_t is tensile strain, and C and m are fatigue regression constants.

Although the uniaxial indirect tensile test addresses some of the shortcomings of the indirect tensile fatigue test on foamed

bituminous mixtures, the test does not eliminate one of the major drawbacks of the indirect tensile fatigue test, which is permanent deformation of the specimen in addition to fatigue damage. This is due to the nature of the test in which permanent axial strain is inevitable, in a similar way to wheel tracking fatigue tests. As the fatigue test results are very sensitive to test type and loading conditions, uniaxial indirect tensile test fatigue lines are plotted in Figure 4 along with indirect tensile fatigue test tests for comparison. The diametral indirect tensile fatigue test was conducted using the Nottingham asphalt tester, performed in accordance with BS DD AFB: 2000 (BSI, 2000) and BS DD AFB: 2003 (BSI, 2003). The test was carried out at a standard temperature of $20 \pm 1^\circ\text{C}$ using 100 ± 3 mm dia. specimens. Although a thickness of 40 ± 2 mm is recommended in the standards, in this study 60 ± 2 mm thick samples were used as it was found difficult to trim the thicker samples to 40 mm because the trimming compromised the integrity of the sample. The test was performed at various stress levels (initial strain levels) at a rate of 40 pulses/min. Each specimen was repeatedly loaded until it failed by cracking or a total vertical deformation of 9 mm had been achieved (as larger permanent deformation would likely compromise reliable measurement of the fatigue behaviour). The target test stress levels were selected to give as wide a range of lives as possible. As can be seen from Figure 4, the

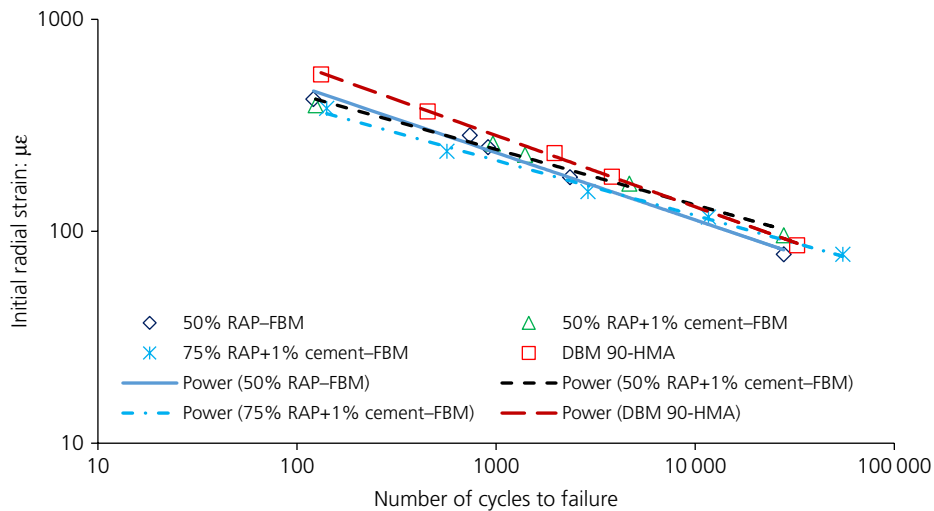


Figure 3. Uniaxial indirect fatigue test results obtained for different mixtures

Table 3. Regression coefficients for fatigue equations from uniaxial test

| Mixture type | C | m | R^2 |
|---|-----------------------|-------|-------|
| 50% RAP-foamed bituminous mixture | 2.00×10^{10} | 3.114 | 0.98 |
| 50% RAP + 1% cement-foamed bituminous mixture | 1.00×10^{12} | 3.774 | 0.98 |
| 75% RAP + 1% cement-foamed bituminous mixture | 9.00×10^{11} | 3.825 | 0.97 |
| DBM90-hot mix asphalt | 2.00×10^{10} | 2.968 | 0.99 |

Offprint provided courtesy of www.icevirtuallibrary.com
Author copy for personal use, not for distribution

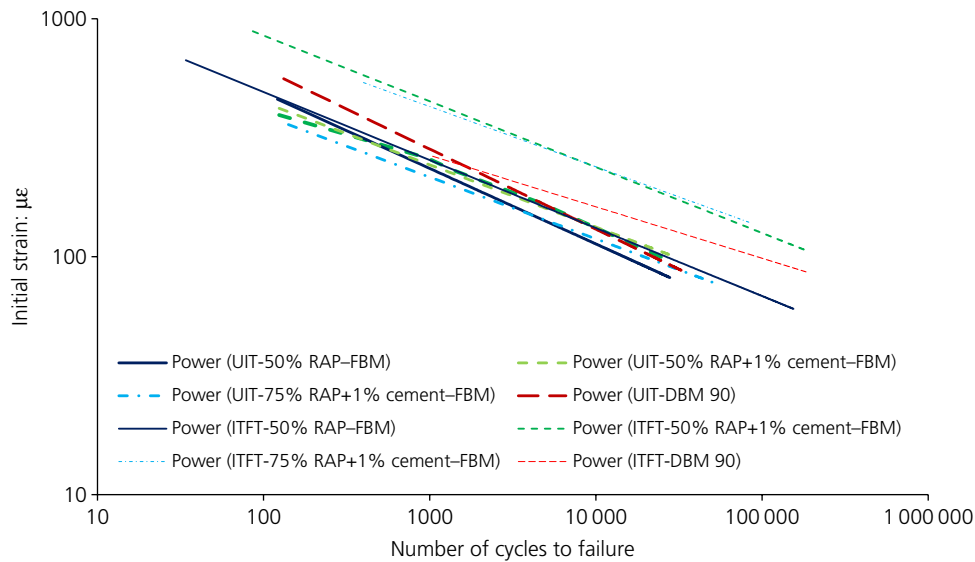


Figure 4. Comparison of fatigue lines obtained from indirect tensile fatigue test and uniaxial indirect tensile

uniaxial indirect tensile test in general resulted in shorter fatigue lives. This could be attributed to the equivalent loading frequency of the tests in addition to other factors such as test type and the difference in accumulated permanent deformation. The indirect tensile fatigue test was required to be performed at ~ 2.5 Hz while the uniaxial indirect tensile test was performed at a loading frequency of 1 Hz.

3.3 Stiffness evolution

There is general agreement on how stiffness is calculated for a test specimen subjected to uniaxial sinusoidal loading (Nunn, 1996). The stiffness modulus under uniaxial stress conditions is defined as the ratio between maximum axial stress and maximum axial strain. However, in the indirect tensile test, the stress system is biaxial and stresses vary throughout the specimen. This means that the stiffness modulus calculation requires analysis of the stress system and this becomes highly complex for non-linear elastic or visco-elastic materials. This is one of the main reasons for adopting the uniaxial test for foamed bituminous mixtures.

Figure 5 shows the first four load cycles of the uniaxial indirect tensile test on a 50% RAP-foamed bituminous mixture. As can be seen from the figure, the applied stress curve and resulting strain curve were at 1 Hz frequency. The ratio of peak stress to peak strain is termed stiffness (S) in this discussion. The stiffness for the entire test duration was calculated accordingly and is plotted in Figure 6 for the 50% RAP-foamed bituminous mixture. Although tests were carried out at five radial

strain levels, for brevity stiffness evolution curves for the three middle strain levels are presented in the figure. As expected, the initial radial strain level significantly affected the stiffness reduction rate. The higher the initial strain level, the shorter the time to reach 50% stiffness. In order to analyse the stiffness evolution independently of the initial strain level, the stiffness data were normalised as shown in Figure 7. For each data point at a specific strain level, the relative time was obtained by dividing the actual number of cycles corresponding to that data point by the number of cycles corresponding to 50% stiffness. As can be seen from Figure 7, the three normalised stiffness curves for the 50% RAP-foamed bituminous mixture followed approximately the same path irrespective of the initial radial strain level. A similar observation is also valid for the other mixtures.

In order to use these trends in pavement analysis and design, the normalised stiffness curves of all the mixtures considered in the study were averaged and polynomial curves were fitted as depicted in Figure 8. It is clear from the figure that the stiffness evolutions of the foamed bituminous mixture and hot mix asphalt are very different. The DBM90 tends to have a three-stage evolution process during the test, similar to four-point bending tests (e.g. Cocurullo *et al.*, 2008). After a rapid reduction in stiffness (phase I), sometimes associated with the internal heating phenomenon, the stiffness decrease becomes more linear (phase II). Fracture occurs in the final stage (phase III) and it is characterised by an acceleration of stiffness decrease. However, this three-stage stiffness evolution was not seen in the foamed bituminous mixtures. The stiffness

Offprint provided courtesy of www.icevirtuallibrary.com
Author copy for personal use, not for distribution

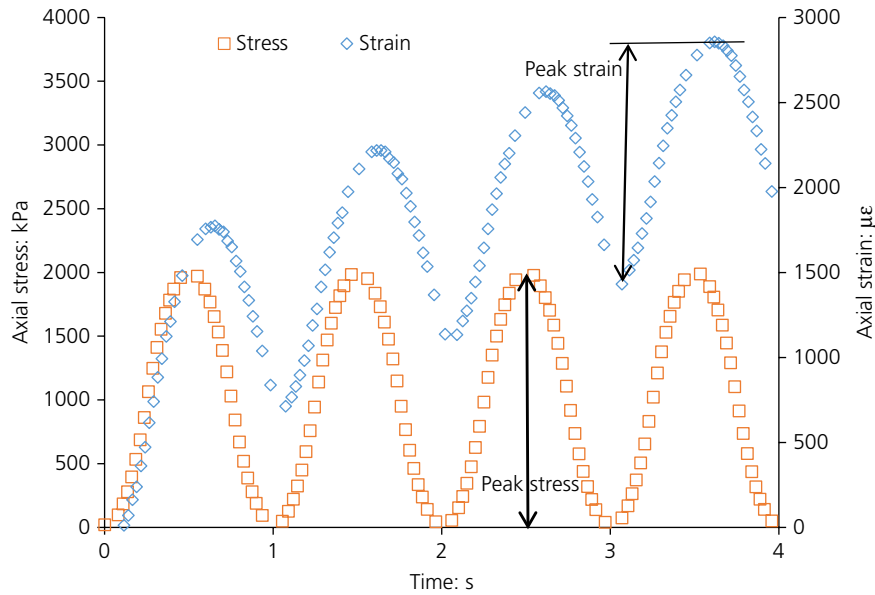


Figure 5. Applied stress and resulting axial strain of 50% RAP-foamed bituminous mixture

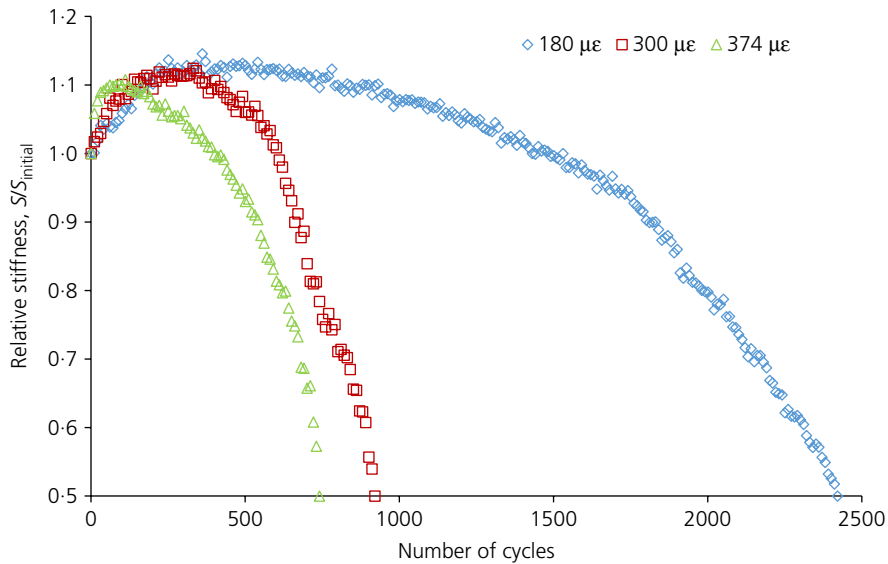


Figure 6. Stiffness evolution curve for 50% RAP-foamed bituminous mixture at different initial radial strain levels

increased rapidly to reach a maximum and then decreased at a slower rate. The maximum for all the mixtures was found to lie between 0.1 and 0.3 of the relative time to reach 50% of stiffness. This increase in stiffness may be associated with densification of the mixtures during the test. This is a logical interpretation as the air void content in the foamed bituminous

mixtures was found to be in the range of 14–18% depending on the mixture type, whereas the average air voids of DBM90 was found to be 5.3%. To verify this explanation, volumetric strain was calculated from axial strain and radial strain measured during the test. The volumetric strain of the 50% RAP-foamed bituminous mixture specimen that was tested at

Offprint provided courtesy of www.icevirtuallibrary.com
Author copy for personal use, not for distribution

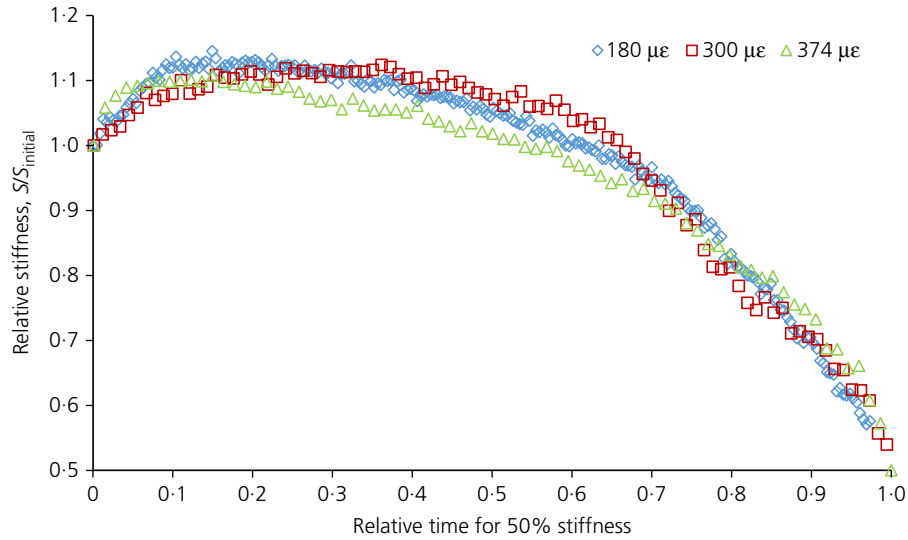


Figure 7. Normalised stiffness reduction curve for 50% RAP-foamed bituminous mixture

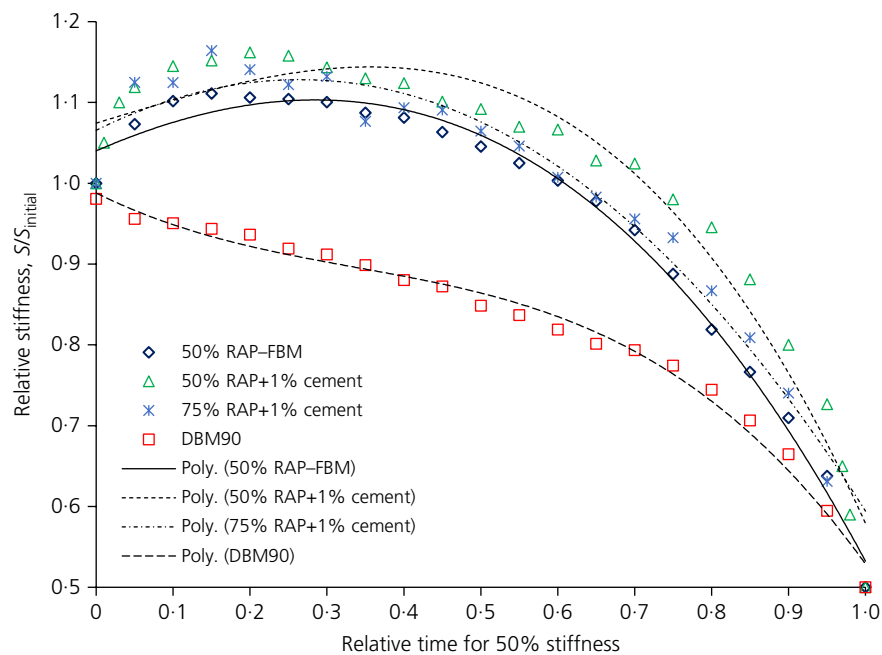


Figure 8. Comparison of stiffness evolution of the mixtures considered in the study

an initial radial strain level of 300 µε is plotted against relative time for 50% stiffness reduction in Figure 9. As can be seen from the figure, the volumetric strain decreased below zero, indicating densification during the initial stage of the test, followed by strain increase.

4. Structural (analytical) design

The mechanistic (analytical)-empirical approach to designing flexible pavements requires two steps. In the first step, the response (stress and strain) of the pavement layers to the wheel loads is calculated using analytical tools. From these data

Offprint provided courtesy of www.icevirtuallibrary.com
Author copy for personal use, not for distribution

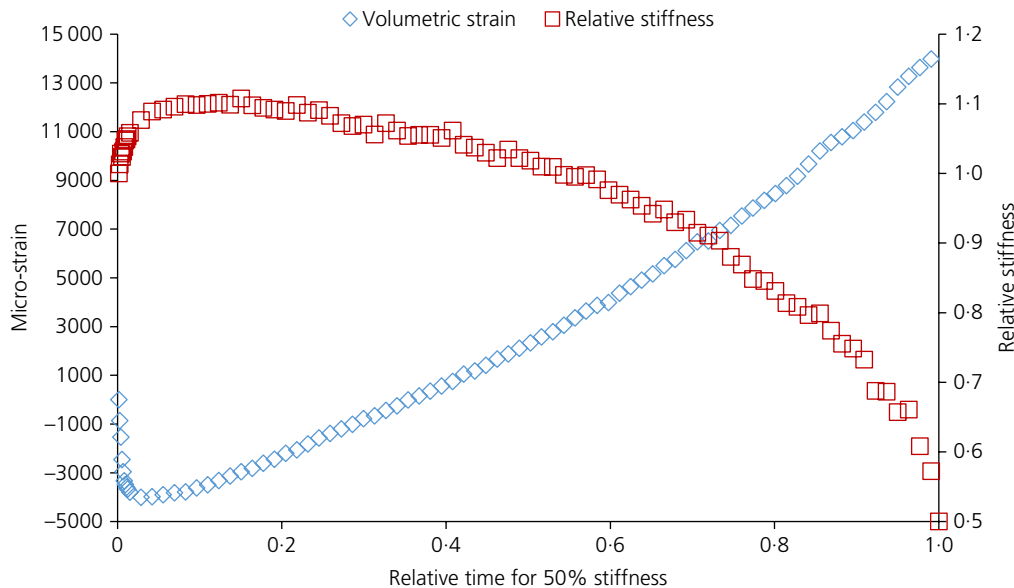


Figure 9. Volumetric strain of 50% RAP-foamed bituminous mixture test at initial radial strain of $300 \mu\epsilon$

critical points are identified. In the second step, these critical responses are compared with the permissible stresses and strains obtained from the performance equation. For design purposes, generally only two locations in the pavement structure are considered for critical stresses and strains. These are the bottom of the base layer and the top of the subgrade where the maximum values of the key parameters develop in most cases. Since this study considers only fatigue, the tensile strain at the bottom of the base layer was used as the design parameter. This is because fatigue cracking of a bituminous layer under repeated wheel loads has been found to depend on the magnitude of tensile strain rather than stress, and therefore this parameter is generally used to characterise the fatigue life of an asphalt pavement, using a fatigue characterisation of the form shown in Equation 1.

Figure 10 shows a flowchart for mechanistic-empirical pavement design against fatigue cracking using the fatigue relationships developed in the previous section. The design process involves the selection of available materials and thicknesses to ensure that the fatigue criterion is satisfied. For the number of load applications expected during the design life of the pavement, the maximum allowable value of each strain criterion has to be determined. As can be seen in the flowchart, the key parameters for flexible pavement design are the cumulative number of standard axle loads for the design life, the design temperature, the properties of the materials used in each layer and the fatigue characteristics of the base layer. As previously discussed, a standard wheel load of 40 kN has been used for analysis purposes.

4.1 Design inputs and analysis

The traffic (wheel load) induced response of pavement layers (stresses and strains) depends on the interaction of layer thicknesses and material properties. Elastic properties are characteristics of importance as they influence the stresses and strains and thus the failure of the pavement layer. Given the non-linear elastic (or visco-elastic) characteristics of foamed bituminous mixtures, strains are non-linear functions of the stress condition. In this study, the analysis was carried out using KENLAYER, an analytical tool that is capable of both linear and non-linear analysis of materials. KENLAYER is an analytical tool for flexible pavements within the KENPAVE computer program developed by Huang (2004). Huang (2004) states that three methods have been incorporated into KENLAYER for non-linear analysis. Method 1, the most accurate but time consuming, was used in this study where the stress-dependent layer is subdivided. Huang (2004) reported that using a non-linear elastic approach and dividing the cold mix layer into sub-layers, each with a unique stiffness, results in higher stress ratios that are better estimates than those obtained by linear elastic calculations. Therefore, the non-linear elastic approach was adopted in this exercise. The other two methods and a detailed description of the capabilities of the program are documented by Huang (2004).

For non-linear elastic analysis using KENLAYER, the parameters of the traditional $K-\theta$ model (k_1 and k_2) are required as presented in Equation 2. To obtain these parameters, triaxial tests were carried out on foamed bituminous mixtures at confining stresses (σ_c) of 50–200 kPa and deviator stresses

Offprint provided courtesy of www.icevirtuallibrary.com
Author copy for personal use, not for distribution

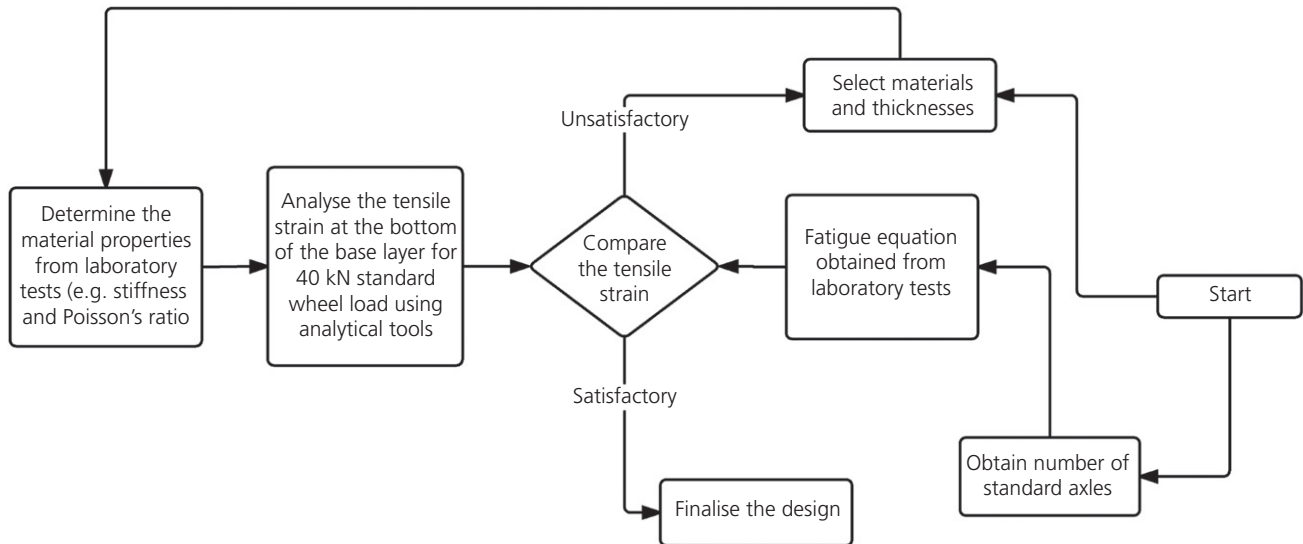


Figure 10. Flowchart for design of flexible pavement against fatigue cracking

(σ_d) of 50–240 kPa, with these stress levels having been determined in preliminary KENLAYER runs. The testing conditions were a temperature of 20°C and a loading frequency of 5 Hz as recommended by Highways England (HD26/06 (HA, 2006)). The control mixture, which was a DBM90, was considered as linear elastic for analysis purposes, with an indirect tensile stiffness modulus value of 3200 MPa. For other layers (sub-base and subgrade) in the pavement structure, hypothetical typical material properties were assumed. The relevant material properties for the pavement layers are detailed in Table 4. The 100 MPa stiffness of subgrade corresponds to 15% CBR converted to stiffness using the relationship recommended by IAN 73/06. From the uniaxial compression tests that were carried out it was found that the Poisson's ratio of the foamed bituminous mixtures considered in the study was in the range 0.2–0.45, independent of the mixture type. An average value of 0.35 was adopted for structural analysis.

$$2. \quad E = k_1 \times \theta^{k_2}$$

where θ is the bulk stress and k_1, k_2 are regression constants determined by statistical analysis of laboratory data.

Non-linear elastic behaviour was considered for base layers with foamed bituminous mixtures and for the sub-base in all cases. For non-linear analysis, the layer was divided into sub-layers of 50 mm thickness. As the KENLAYER non-linear analysis forms an iterative approach, a seed stiffness value was required for each case. Seed stiffness values of 500–1200 MPa were used for the foamed bituminous mixtures depending on the number of sub-layers. For each iteration, a stiffness value for each sub-layer is calculated by KENLAYER based on the magnitude at the mid-depth of the sub-layer of stress obtained in the previous iteration. This is repeated by the KENLAYER program until the stiffness converges to a specific tolerance limit. The outputs from the KENLAYER analysis are vertical, horizontal and shear stresses and strains and vertical displacement values. The output file also includes the stiffness values for each of the sub-layers.

The significance of the non-linear analysis approach for foamed bituminous mixtures can be determined in Figure 11.

Table 4. Pavement layer material properties

| Material | Layer | Density: kg/m ³ | Poisson's ratio | Elastic behaviour | Stiffness/ k_1 and k_2 : MPa |
|---------------------|-----------|----------------------------|-----------------|-------------------|----------------------------------|
| HRA(40/60) | Surfacing | 2400 | 0.35 | Linear | 3100 |
| DBM90 | Base | 2400 | 0.35 | Linear | 3200 |
| 50% RAP | Base | 2180 | 0.35 | Non-linear | 424 and 0.413 |
| 50% RAP + 1% cement | Base | 2180 | 0.35 | Non-linear | 678 and 0.351 |
| 75% RAP + 1% cement | Base | 2140 | 0.35 | Non-linear | 707 and 0.372 |
| Unbound | Sub-base | 2000 | 0.35 | Non-linear | 50 and 0.55 |
| Unbound | Subgrade | 1800 | 0.4 | Linear | 100 |

Offprint provided courtesy of www.icevirtuallibrary.com
Author copy for personal use, not for distribution

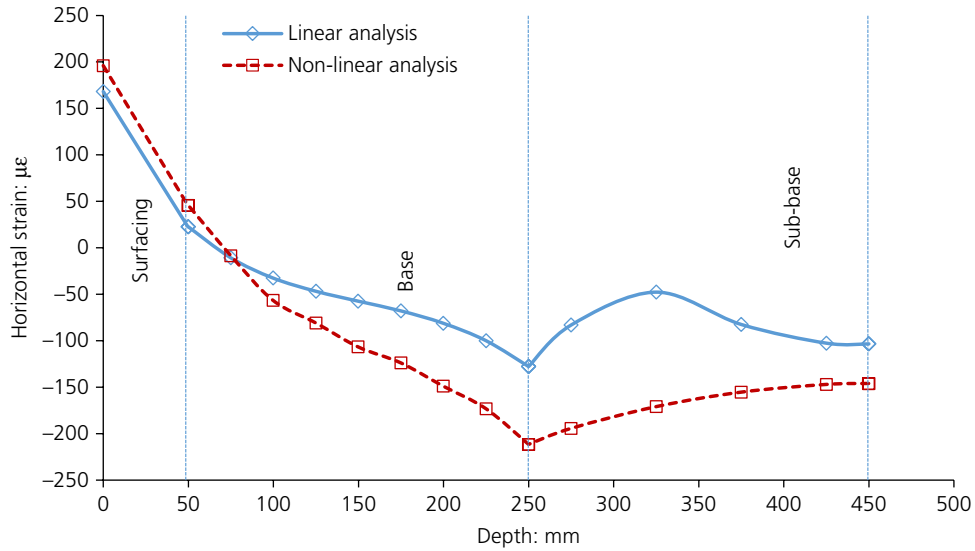


Figure 11. Horizontal strain distribution through pavement structure for 50% RAP-foamed bituminous mixture

The figure shows the distribution of horizontal strain through the depth of the pavement. Analysis was carried out considering a 50% RAP-foamed bituminous mixture first as a non-linear material and then as a linear material. For the linear analysis case, the stiffness value at 20°C (found to be 2550 MPa) was used. For the non-linear analysis, the parameters used were as listed in Table 4. As can be seen from Figure 11, within the surface layer (up to a depth of 50 mm) the horizontal strain distributions are not very different.

However, in the base and sub-base layers, the horizontal strain distribution is considerably different using non-linear analysis when compared with linear analysis. The higher values of strain for non-linear analysis are due to the stress-dependent stiffness values of foamed bituminous mixtures. Figure 12 presents vertical stress distributions in the pavement induced by a standard wheel load. As can be seen from the figure, the vertical stress decreases with depth within the pavement. At lower stress levels these materials tend to have low

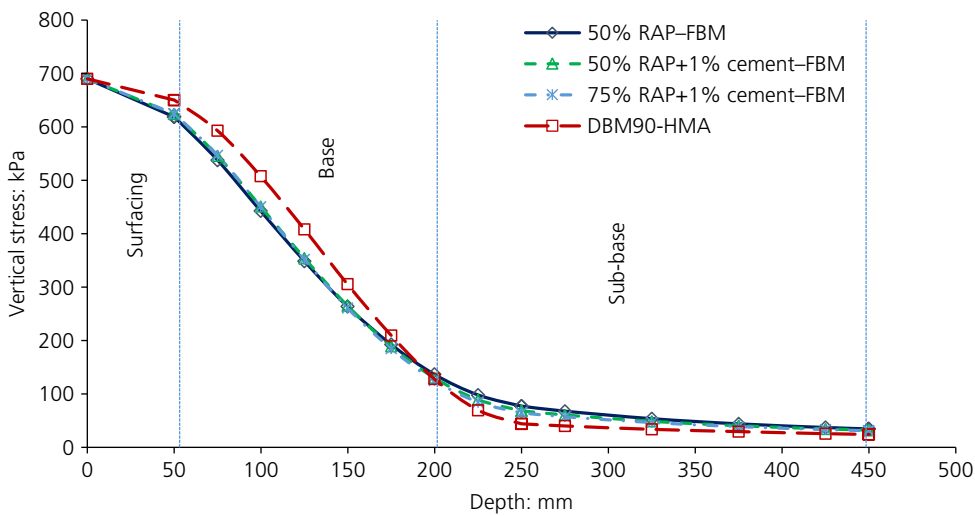


Figure 12. Vertical stress distribution through pavement structure

Offprint provided courtesy of www.icevirtuallibrary.com
Author copy for personal use, not for distribution

stiffness due to their non-linearity (similar to granular material).

4.2 Cumulative damage approach

In the traditional pavement design approach, fatigue life is determined assuming that the base layer will have a constant stiffness throughout the life of the pavement. The fatigue life of a pavement layer in this approach is defined as the number of standard wheel loads it can sustain at a certain strain level. The magnitude of the maximum permissible strain is established by means of laboratory tests resulting in fatigue lines of the form presented in Equation 1 and ‘transferred’ to field performance by a ‘shift factor’. To obtain the design thickness of the pavement layers, layer thicknesses are adjusted until the strain criterion is satisfied. Including the shift factor, K , Equation 1 can be re-written as follows

$$3. \quad N_f = K \times \left(\frac{1}{\varepsilon_t}\right)^m$$

The shift factor K is usually derived using performance data collected from the field or from full-scale experimental pavements exposed to realistic loading conditions. Therefore, the shift factor naturally accommodates effects such as stiffness loss due to traffic loads, stiffness gain due to curing and temperature effects during the life of the pavement along with load characteristics. Thus, the shift factor K is usually a constant that accounts for all the individual factors that influence pavement performance, which includes load induced stiffness evolution. However, as shown in Figure 8, the load induced stiffness evolution in foamed bituminous mixtures follows a considerably different trend from that of DBM90, suggesting that the shift factor obtained for hot mix asphalt base pavements may not be appropriate for foamed bituminous mixtures.

To account for the stiffness evolution, an iterative approach recommended by Oliveira (2008) was adopted to accommodate layer stiffness evolution in the design. This approach approximates the load induced stiffness evolution in predefined intervals and sums the damage over each interval (Miner’s law). For this, the stiffness evolution curve was divided into equal time intervals. Within each interval the average stiffness value was used as the input value for determining the strain level in the pavement, which was assumed constant during that interval. This procedure is straightforward if linear elastic behaviour is assumed as stiffness values are input directly into the KENLAYER. However, in this study non-linear elastic behaviour was assumed for foamed bituminous mixtures with non-linear parameters k_1 and k_2 as inputs and the assumption has been made that k_1 (stiffness modulus constant) follows the

stiffness evolution trend and k_2 (stress-dependent parameter) remains constant throughout. For each strain level the corresponding fatigue life was estimated from the fatigue equation of each mixture, assuming a constant strain during each interval. However, since only a portion of the fatigue life is consumed during each interval, the cumulative fatigue life was calculated by adding the lives consumed during all the intervals (Miner’s law). This iterative procedure approach is illustrated in the flowchart in Figure 13.

It has to be noted that, in this iterative approach, the shift factor K_L , which accounts for the load induced damage during the pavement life, is used for calculation of the fatigue life for each interval. Thus, the fraction of life that expires in the interval i is given by following equation

$$4. \quad N_i = K_L \times C \times (1/\varepsilon_i)^m$$

where ε_i is the tensile strain obtained at the bottom of the base for a constant stiffness in each interval.

Both the approaches should produce the same pavement life if the fatigue equation is calibrated from performance data from full-scale experimental or actual road pavements. If the pavement life is divided into n equal intervals then the cumulative damage approach results in a pavement life of N . If the road is subjected to equal amounts of traffic in each interval as in the tests then N will be equal to

$$5. \quad N = \frac{1}{n} \times \sum_1^n K_L \times \left(\frac{1}{\varepsilon_i}\right)^m$$

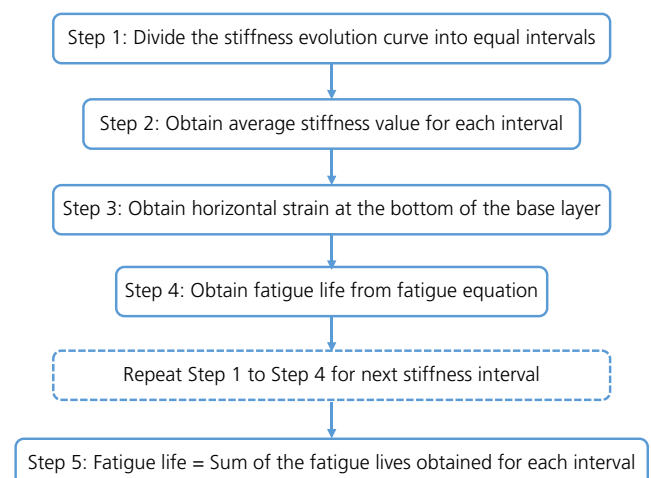


Figure 13. Flowchart for cumulative fatigue life approach (design)

Offprint provided courtesy of www.icevirtuallibrary.com
Author copy for personal use, not for distribution

Substituting Equation 2 into the above equation and rearranging

$$6. \quad \frac{K}{K_L} = \frac{1}{n} \times \varepsilon^m \times \sum_{i=1}^n (1/\varepsilon_i)^m$$

To determine the effectiveness of the cumulative damage approach, a normalised life determined by both approaches is calculated. Figure 14 shows the horizontal tensile strain obtained for each interval for a standard wheel load and a constant stiffness within each interval. The fatigue life from the traditional approach is determined assuming a constant stiffness throughout the life and normalised to hot mix asphalt fatigue life to obtain the relative life. The results are presented in Figure 15. As can be seen in the figure, the traditional approach gives conservative results for foamed bituminous mixtures compared with the cumulative damage approach in which load induced stiffness evolution is taken into account. This indicates that the shift factor ‘K’ should be higher for foamed bituminous mixture than hot mix asphalt, assuming all other factors such as curing have the same effect on both the mixtures. This can be explained by the relation between K and K_L. The ratio K/K_L can be determined by Equation 6. The strain inputs for each interval are the same values as obtained for relative fatigue life (Figure 14). The K/K_L values for the 50% RAP-foamed bituminous mixture, the 50% RAP+1% cement-foamed bituminous mixture, the 75% RAP+1% cement-foamed bituminous mixture, the 75%

RAP+1% cement-foamed bituminous mixture and DBM90 were found to be 0.99, 1.06, 1 and 0.77, respectively. Thus, the shift factor K for foamed bituminous mixtures should be 25–35% higher than that for hot mix asphalt. This is based on the assumption that all other pavement performance factors have the same effect on the pavements for both the mixtures.

In practice, the shift factor K varies significantly based on the type of laboratory loading, frequency of loading, test temperature and so on. For flexible pavements, the shift factor ranges from 2 to 440 according to different researchers depending on the test conditions (Oliveira *et al.*, 2008). In the present project, fatigue tests were conducted at 1 Hz frequency at 20°C, which are considered to be very conservative testing conditions. Therefore, a shift factor of 400 has been assumed. The resulting shift factors (K values) to be used in Equation 3 are 507, 548 and 520, respectively, for the 50% RAP-foamed bituminous mixture, the 50% RAP+1% cement-foamed bituminous mixture, and the 75% RAP+1% cement-foamed bituminous mixture. A similar approach was followed to obtain K/K_L values for hypothetical pavement sections with 250 and 300 mm base thicknesses. It was found that the ratio is not sensitive to thicknesses.

The resulting fatigue equations derived from Equation 1 are as in Equations 7, 8, 9 and 10, respectively, for the 50% RAP-foamed bituminous mixture, the 50% RAP+1% cement-foamed bituminous mixture, the 75% RAP+1% cement-foamed bituminous mixture and DBM90. Figure 16 presents

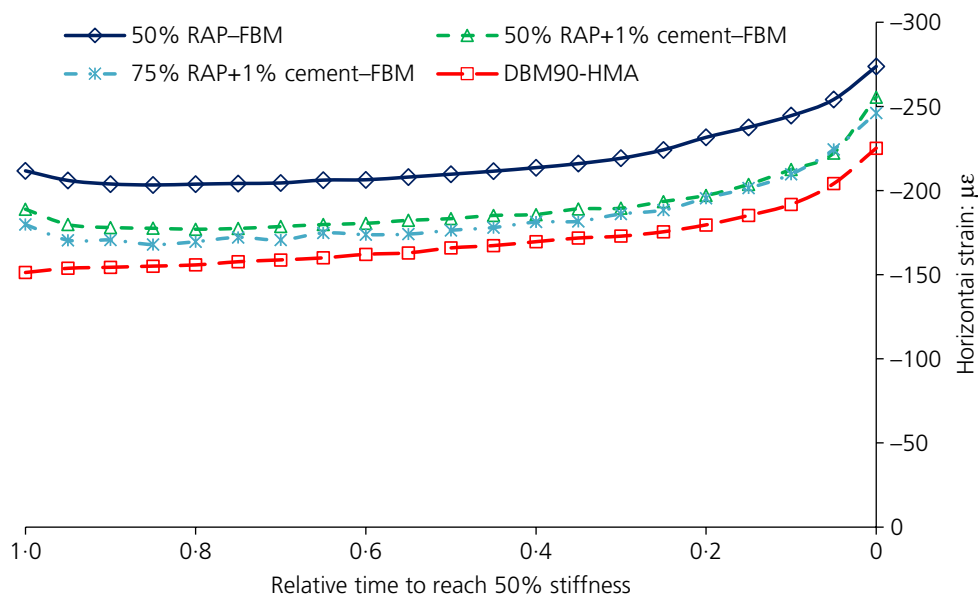


Figure 14. Horizontal strains (tensile) obtained at the bottom of the base layer

Offprint provided courtesy of www.icevirtuallibrary.com
Author copy for personal use, not for distribution

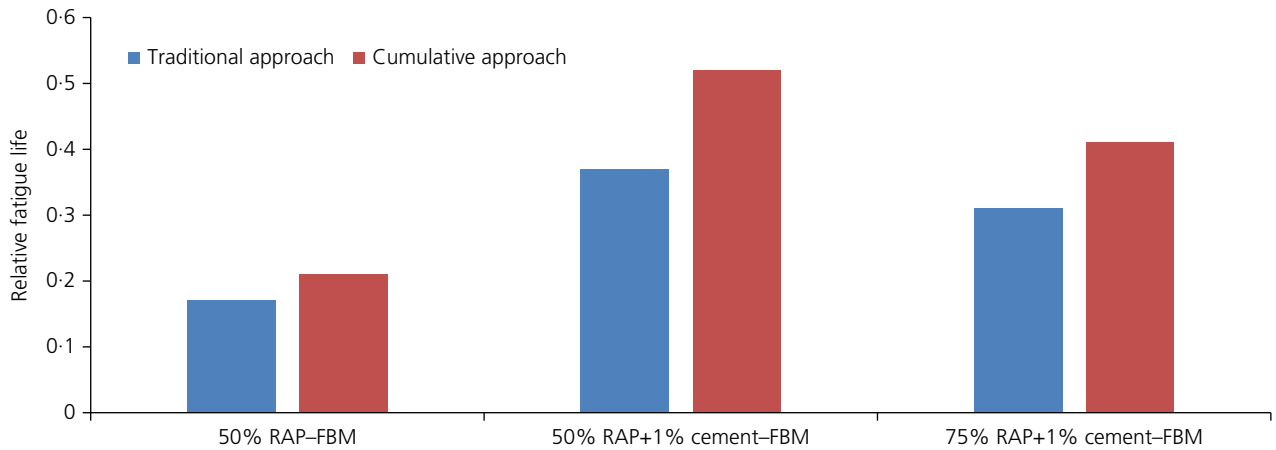


Figure 15. Relative fatigue life to hot mix asphalt of foamed bituminous mixtures pavements

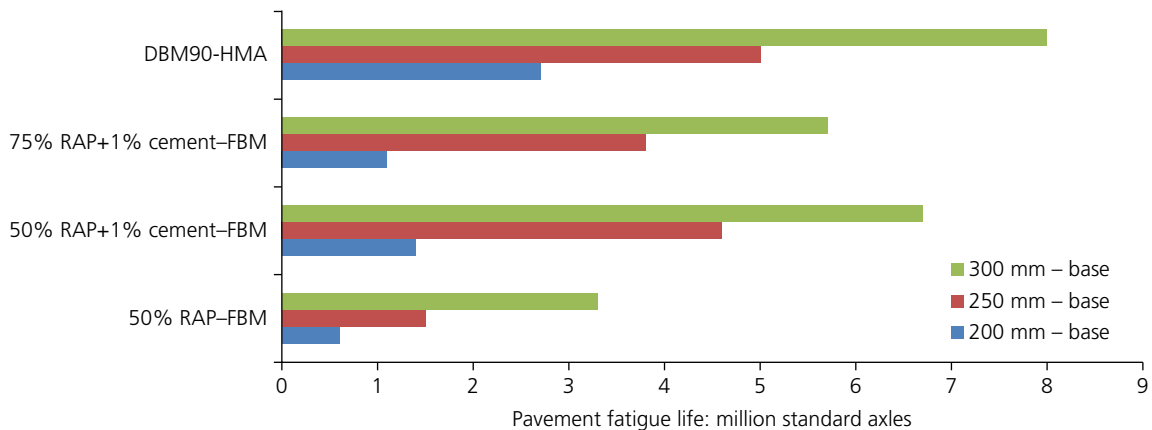


Figure 16. Fatigue life of pavements with different bases thicknesses

the results of fatigue lives for each mixture considered in the study and for different base thicknesses. As can be seen from the figure, the fatigue life of foamed bituminous mixtures is comparable with hot mix asphalts, particularly for pavements with thicker bases

$$7. \quad N_f = 1.04 \times 10^{13} \times \left(\frac{1}{\varepsilon_t}\right)^{3.114} \quad \text{for 50\% RAP}$$

– foamed bituminous mixture

$$8. \quad N_f = 5.37 \times 10^{14} \times \left(\frac{1}{\varepsilon_t}\right)^{3.774} \quad \text{for 50\% RAP + 1\% cement}$$

– foamed bituminous mixture

$$9. \quad N_f = 4.64 \times 10^{14} \times \left(\frac{1}{\varepsilon_t}\right)^{3.825} \quad \text{for 75\% RAP + 1\% cement}$$

– foamed bituminous mixture

$$10. \quad N_f = 8 \times 10^{13} * \left(\frac{1}{\varepsilon_t}\right)^{2.968} \quad \text{for DBM90}$$

5. Conclusions

This study has introduced a laboratory fatigue test, the ‘uniaxial indirect tension test (uniaxial indirect tensile)’ for foamed bituminous mixtures and a rational structural design approach, the ‘cumulative damage approach (cumulative damage)’, for

Offprint provided courtesy of www.icevirtuallibrary.com
Author copy for personal use, not for distribution

pavements incorporating foamed bituminous mixtures. The uniaxial indirect tensile test is believed to address some of the limitations of the traditional fatigue tests of foamed bituminous mixtures. The test also enables a stiffness evaluation curve to be obtained in addition to the data required to establish fatigue lines (equations). It was deduced from the tests that the load induced stiffness evolutions of foamed bituminous mixtures and hot mix asphalt are very different. The hot mix asphalt tends to have a three-stage evolution process during the test, similar to four-point bending tests. However, this three-stage stiffness evolution was not identified for the foamed bituminous mixtures that were considered in the study. The stiffness increased rapidly to reach a maximum and then decreased at a slower rate. These stiffness evolution curves are used as input for the cumulative damage approach. The cumulative damage approach was carried out on a purely comparative basis using a single pavement structure, and different mixtures were studied. The results showed that the traditional design approach yields conservative outcomes for pavements with foamed bituminous mixtures if the same transfer function (shift factor) used for hot mix asphalt is applied. The results also showed that, if all the other factors influencing performance of pavements with foamed bituminous mixture and hot mix asphalt are the same, the shift factor for foamed bituminous mixtures should be 25–35% higher than for hot mix asphalt. The K_1/K values determined from this study can be used to calibrate the shift factors to be used in the traditional design approach in the absence of performance data for pavements with foamed bituminous mixtures. This study is limited to evaluating the effect of load induced stiffness evolution on pavement design life. A similar approach could be adopted for predicting the influence of stiffness evolution due to curing on pavement life. It is well established that foamed bituminous mixtures gain considerable strength/stiffness with time. It is possible that curing stiffness evolution could have a significant influence on fatigue life.

REFERENCES

- BSI (2000) DD AFB: Method for the determination of the fatigue characteristics of bituminous mixtures using indirect tensile fatigue (Draft for Development). British Standard Institute, London, UK.
- BSI (2003) DD AFB: Method for the determination of the fatigue characteristics of bituminous mixtures using indirect tensile fatigue (Draft for Development). British Standard Institute, London, UK.
- BSI (2005) BS 4987-1: Coated macadam (asphalt concrete) for roads and other paved areas. Specification for constituent materials and for mixtures. British Standard Institute, London, UK.
- Cocurullo A, Airey GD, Collop AC and Sangiorgi C (2008) Indirect tensile versus two-point bending fatigue testing. *Proceedings of the Institution of Civil Engineers – Transport* **161(4)**: 207–220, <https://doi.org/10.1680/tran.2008.161.4.207>.
- HA (Highways Agency) (2006) *HD26: Design Manual for Roads and Bridges, Volume 7*. HA, London, UK.
- Huang YH (2004) *Pavement Analysis and Design*. Pearson Prentice Hall, Upper Saddle River, New Jersey, US.
- IAN (Interim Advice Notes) (2006) IAN 73: Design of Pavement Foundations, Design Manual for Roads and Bridges, Highways Agency, London, UK.
- Jenkins KJ (2000) *Mix Design Considerations for Cold and Half-Warm Bituminous Mixes with Emphasis on Foamed Bitumen*. PhD thesis, University of Stellenbosch, Stellenbosch, South Africa.
- Jenkins KJ, Molenaar AAA, de Groot JLA and van de Ven MFC (2002) Foamed asphalt produced using warmed aggregates. *Journal of the Association of Asphalt Paving Technologists* **71**: 444–478.
- Kim YR (2009) *Modeling of Asphalt Concrete*. McGraw-Hill Professional Publication, New York, NY, USA.
- Kuna K (2014) *Mix Design Considerations and Performance Characteristics of Foamed Bitumen Mixtures (Foamed Bituminous Mixtures)*. PhD thesis, University of Nottingham, Nottingham, UK.
- Kuna K, Airey G and Thom N (2014) Laboratory mix design procedure for foamed bitumen mixtures. *Transportation Research Record* **2444**: 1–10.
- Kuna K, Airey G and Thom N (2016) Mix design considerations of foamed bitumen mixtures with reclaimed asphalt pavement material. *International Journal of Pavement Engineering*: 1–14.
- Long F and Theyse H (2004) Mechanistic empirical structural design models for foamed and emulsified bitumen treated materials. In *Proceedings of the 8th Conference on Asphalt Pavements for Southern Africa, Sun City, South Africa*.
- Long F, Theyse HL, Robroch S and Liebenberg J (2002) Performance models for deep in situ recycled, bitumen stabilised pavements under accelerated traffic. In *Proceedings of the 9th International Conference on Asphalt Pavements, Copenhagen, Denmark*.
- Nunn M (1996) *The Characterisation of Bituminous Macadam by Indirect Tensile Stiffness Modulus*. TRL, Wokingham, UK, Report 160.
- Oliveira JRM (2008) *Grouted macadam: Mechanical characterization for pavement design*. PhD Thesis, University of Nottingham, Nottingham, UK.
- Oliveira JRM, Thom NH and Zoorob SE (2008) Design of pavements incorporating grouted macadam. *Journal of Transportation Engineering* **134(1)**: 7–14.
- Ramanujam JM and Jones JD (2007) Characterization of foamed-bitumen stabilisation. *International Journal of Pavement Engineering* **8(2)**: 111–122.
- Thom N (2013) *Principles of Pavement Engineering*, 2nd edn. ICE Publishing, London, UK.
- Van de Ven MFC, Jenkins KJ, Voskuilen JLM and Van den Beemt R (2007) Development of (half-) warm foamed bitumen mixes: state of the art. *International Journal of Pavement Engineering* **8(2)**: 163–175.

How can you contribute?

To discuss this paper, please email up to 500 words to the editor at journals@ice.org.uk. Your contribution will be forwarded to the author(s) for a reply and, if considered appropriate by the editorial board, it will be published as discussion in a future issue of the journal.

Proceedings journals rely entirely on contributions from the civil engineering profession (and allied disciplines). Information about how to submit your paper online is available at www.icevirtuallibrary.com/page/authors, where you will also find detailed author guidelines.